Desalination and Water Treatment
www.deswater.com

doi:10.5004/dwt.2018.22924

125 (2018) 26–31
September

Treatment of distillation residue waste liquid from NPEOs by hydrothermal carbonization process for resource recovery

Jiexiu Hao[a], Wenqi Zhang[a,*], Gang Xue[b], Pinhua Rao[a], Runkai Wang[a]

[a]*College of Chemistry and Chemical Engineering, Shanghai University of Engineering Science, Shanghai, 201620, China, Tel. +86-173-1752-0860, email: 1013211782@qq.com (J. Hao), Tel. +86-159-0074-6789, Fax +86-021-6779-1214, email: zhangwenqi_hit@163.com (W. Zhang), Tel. +86-021-6779-1211, email: raopinhua@hotmail.com (P. Rao), Tel. +86-136-2172-0394, email: wrk007@163.com (R. Wang)*

[b]*College of Environmental Science and Engineering, Donghua University, Shanghai, 201620, China, Tel. +86-021-6779-2558, email: xuegang@dhu.edu.cn (G. Xue)*

Received 20 November 2017; Accepted 6 August 2018

ABSTRACT

Wastewater from high-concentration nonylphenol polyethoxylates (NPEOs) is often treated by distillation, and approximately 3% vol distillation residue waste liquid is produced from NPEOs; this waste liquid is not easily disposable. A simple route was developed, and the waste liquid was used to fabricate porous carbon via hydrothermal carbonization (HTC). The results showed that the porous carbon could be obtained at low or high temperatures (160–220°**C**). As the temperature decreased, the reaction time increased. The porous carbon samples had a rough surface and micro-mesoporous structure. The largest Brunauer-Emmett-Teller (BET) surface area (S_{BET}) of the porous carbon could reach 439 $m^2\ g^{-1}$ at a temperature of 220°C at 0.5 h. Functional groups containing C–H, C=O and S=O existed on the surface of the porous carbon.

Keywords: NPEOs waste liquid; Porous carbon; Hydrothermal carbonization; Resource recovery

1. Introduction

Nonylphenol polyethoxylates (NPEOs) are nonionic surfactants largely used in many agricultural and industrial applications, and approximately 60% of NPEOs produced were estimated to enter the aquatic environment finally via various pathways [1]. NPEOs can be degraded into nonylphenol (NP) and short chain NPEOs in a water body, which are more oleophilic, more persistent and more toxic for fishes and other aquatic organisms [2–4].

Currently, many conventional processes are used to treat low-concentration NPEOs in water, such as activated carbon adsorption [5,6], electrochemical [7], advanced oxidation process (AOP) [8] and biological methods [9]. The above mentioned processes are invalid for treating the waste liquid from NPEOs due to its high concentration and strong foaming property.

Hydrothermal carbonization (HTC) is a process that converts wet biomass into a highly carbonaceous product under moderate temperatures (130~250°**C**) and autogenous pressures [10–12]. Feedstock used includes manure [13,14], herbaceous waste [15,16], municipal waste [17–19], algae [20–22], wet grains [23–25] and others. In recent years, the carbonization of organic pollutants by this process has attracted attention. Some researchers had used the HTC for olive mill wastewater (OMW) treatment and obtained hydrochar at 220°**C** for 14 h successfully [26]. It was also reported that poly(vinyl chloride) (PVC) could be completely dechlorinated in the HTC process at operating temperature above 235°**C** [27]. The degree of degradation of 12 organic compounds from various classes, consisting of pharmaceuticals, pesticides, and industrial chemicals, was analyzed after hydrothermal treatment at 200°**C** for 4 or 16 h, or 255°**C** for 16 h; the results showed that the HTC process had a significant potential to degrade organic pollutants [28]. In our previous work, hydrochar was prepared

*Corresponding author.

via HTC using waste liquid from NPEOs, but the specific surface area of the hydrochar was small and could only be used as alternative fuel [29]. Then, hydrochar with a higher specific surface area was prepared by increasing the ratio of sulfuric acid (10 mL H_2SO_4 per 5 mL of NPEO waste liquid). This study attempts to fabricate porous carbon with high specific surface area by HTC in the optimization of experimental conditions.

2. Experimental

2.1. NPEO waste liquid

The NPEO waste liquid was supplied by a chemical enterprise in China. The total solid (TS) of the waste liquid was measured to be 60 wt% by the gravimetric method, according to standard methods. The chemical oxygen demand (COD) of the waste liquid was 1000 g L^{-1}. More than 60% of organic components of the waste liquid was NPEO, and the remaining components included some complex intermediates produced in the production of polytetrafluoroethylene (PTFE), including nano-PTFE particles. The concentration of metal ions is listed in Table 1.

2.2. Preparation of porous carbon

HTC experiments were performed in a 100 mL polyphenylene (PPL)-lined stainless-steel autoclave reactor (Yanzheng, Shanghai, China). In each experiment, 5 mL of NPEO waste liquid was pipetted into the reactor, 10 mL of 98% sulfuric acid was then added to the reactor. The reaction vessel was sealed and heated to the desired temperature (160–220°**C**) under autogenous pressure (0.3–0.6 MPa). The heating rate was set at approximately 8°**C**/min. After the heating stage, the autoclave was kept at the final preset temperature for the desired reaction time. The reaction temperatures and reaction times are presented in Table 2.

As the reaction time reached, the reactor was cooled down to room temperature. The hydrochar was washed ten times with 20 mL distilled water, totaling 200 mL. Then, the hydrochar was dried in an oven at 120°C for 2 h. The yield of hydrochar ($Y_{hydrochar}$) and the consumption of sulfuric acid (SA_c) were calculated based on the following equations, respectively.

$$Y_{hydrochar}(\%) = \frac{W_{hydrochar}}{W_{TS}} \times 100 \quad (1)$$

$$SA_c = SA_d - SA_r \quad (2)$$

where $Y_{hydrochar}$ – hydrochar yield; $W_{hydrochar}$ – dried hydrochar weight; W_{TS} – the weight of TS in waste liquid; SA_c – consumption of sulfuric acid; SA_d – dosage of sulfuric acid; and SA_r – sulfuric acid residue in the washing water.

The bulk density of hydrochar was measured according to standard methods.

The sulfuric acid residue in the washing water and the COD of the washing water were measured by acid-base titration and potassium dichromate method, respectively, according to standard methods issued by the State Environmental Protection Administration of China (2002).

Table 1
Metal ion concentration in the NPEO waste liquid

Metal ions	Concentration (mg L^{-1})
Al	204.81
Ba	329.06
Cd	225.64
Co	179.97
Cr	208.23
Pb	322.82
Fe	430.79
Na	15977.5

Table 2
Experimental conditions of the HTC process

Sample	Temperature (°C)	Reaction time (h)
H-220	220	0.5
H-200	200	0.5
H-180	180	0.5
H-160	160	0.5
H-160-4	160	4
H-160-6	160	6

The concentration of metal ions in the waste liquid was analyzed using inductively coupled plasma analysis (ICP) (Varian 725–ES, Australia).

2.3. Properties characterization

The morphology and structure of the hydrochar were characterized using Scanning electron microscope (SEM) (HITACHI S-3400, Japan). N_2 adsorption-desorption isotherms were collected on Micromeritics ASAP 2460 at the temperature of 77 K, from which, the surface area (S_{BET}), pore volume (V_p) and pore diameter (D_p) were determined by applying the Brunauer-Emmett-Teller (BET) and Barrett-Joyner-Halenda (BJH) models from the desorption branches. The functional groups on the surface of the hydrochar were investigated with a Fourier-transform infrared spectrometer (FTIR) (Nicolet AVATAR 370, USA) in the infrared range between 4000 and 400 cm^{-1}.

3. Results and discussion

3.1. HTC results in different conditions

The results showed that NPEO waste liquid could be completely converted to hydrochar without any waste liquid remaining under the designed experimental conditions. The yield, the bulk density of hydrochar, the consumption of sulfuric acid and the COD of the washing water of the different hydrochar samples are listed in Table 3.

The main functions of sulfuric acid in the reaction were dehydration and oxidation. The addition of sulfuric acid was greatly beneficial to the carbonation of NPEO waste

Table 3
The yield, the bulk density of hydrochar, the consumption of sulfuric acid and the COD of washing water

Sample	Yield of hydrochar (wt%)	Bulk density of hydrochar (mg cm^{-3})	Consumption of sulfuric acid (mol)	COD of washing water (mg L^{-1})
H-220	67	114	0.11 (59.78%)	504
H-200	86	187	0.06 (32.61%)	517
H-180	94	228	0.05 (27.17%)	937
H-160	22	244	0.04 (21.74%)	3430
H-160-4	68	172	0.05 (27.17%)	909
H-160-6	85	149	0.09 (48.91%)	522

liquid. The waste liquid was not carbonized at 200°C for 24 h without sulfuric acid as an additive. Furthermore, the consumption of sulfuric acid had a great influence on the yield, the bulk density of hydrochar, the COD of washing water, and even the structure of hydrochar. From Table 3, with the decrease of temperature in the range of 220–180°C under the same reaction time (0.5 h), it could be seen that the consumption of sulfuric acid decreased, corresponding to the yield, the bulk density of hydrochar and the COD of the washing water increased. The yield and the bulk density of hydrochar increased, indicating that hydrochar became denser with the decrease of the temperature. The reduction in consumption of sulfuric acid was detrimental to the formation of porous carbon. The increase of COD of the washing water indicated that the organic components involved in the formation of hydrochar decreased with the decrease of the temperature.

To investigate the effect of the different reaction time on the reaction process under the same temperature, the experiments were conducted at 160°C for 0.5 h, 4 h and 6 h, respectively. The results showed that the yield of H-160 decreased sharply to 22 wt%, but the bulk density increased compared to H-180, indicating that the ratio of carbonization was low. Meanwhile, the consumption of sulfuric acid decreased, and the COD of the washing water had a steep rise. With the increase of the reaction time under this temperature (H-160-4 and H-160-6), the consumption of sulfuric acid increased; and the yield, the bulk density of hydrochar and the COD of the washing water decreased gradually. It was assumed that at a certain temperature range, good carbonization results could be obtained by prolonging the reaction time or increasing the reaction temperature.

3.2. SEM

The surface morphologies of the hydrochar are shown in Fig. 1. For H-220, H-200 and H-160-6, the particles were uniformly dispersed with the particle size of 1–2 μm. Samples H-180, H-160 and H-160-4 were agglomerate with inhomogeneous particle size. Under different temperature conditions, the broken degree of the particle surface was different. It seemed that a severe alteration occurred under the high- temperature condition. When the temperature was lower (H-160), the surface of particles was clean and smooth; as the reaction time increased, the alteration of some particles occurred, but there were still some coarse aggregates (H-160-4). Then, the particles were broken and dispersed uniformly, and the surface alteration was more substantial (H-160-6). It was speculated that the alteration also occurred in the interior of the particles, thus affecting the morphology and structure of the hydrochar.

3.3. Porosity

The N_2 adsorption–desorption isotherms in Fig. 2 illustrate that all the hydrochar showed the typical type-I sorption isotherms with an obvious H3 hysteresis loop located at the relative pressure (P/P_0) ranging from 0.2 to 1.0, which was usually considered to be indicative of adsorption in micro pores or meso pores with pore sizes close to the micro pore range, according to the IUPAC classifications [30]. Their corresponding pore size distribution curves revealed that the average pore diameter of the hydrochar was concentrated in the mesoporous range close to micro pore. Based on the N_2 adsorption–desorption isotherms, the S_{BET}, V_P and D_P (see Table 4) was calculated by applying the BET and BJH models, respectively. It was observed that the S_{BET} of H-220, H-200 and H-160-6 were 439 $m^2 g^{-1}$, 329 $m^2 g^{-1}$ and 388 $m^2 g^{-1}$, respectively, which were larger than H-180, H-160 and H-160-4. The reason was that the H-220, H-200 and H-160-6 had smaller D_p and larger V_p. The biggest surface area of the porous carbon (439 $m^2 g^{-1}$) was larger than the hydrochar prepared by HTC of many biomasses and organic matters with higher temperature and longer reaction time [14,16,27].

3.4. FTIR

The surface functional groups were characterized by FTIR spectra in Fig. 3.

For all the hydrochar samples, the band at 3400 cm^{-1} corresponding to the O–H (hydroxyl or carboxyl) stretching vibration indicated that large numbers of –OH groups were on the hydrochar surface [31]. The band at 1700 cm^{-1} implied the stretching vibration of C=O in ketone and amide groups [32]. The C=C stretching vibration in the spectrum was found to be 1615 cm^{-1} [33]. The S=O stretching vibration at 1200–1040 cm^{-1} related to sulfonic acid group [34], which suggested the introduction of sulfonic acid group in the HTC process. The band at 880 cm^{-1}, which was attributed to aromatic C–H out-of-plane bending vibrations, indicated that aromatization (including aldol condensation and dehydration) occurred [35].

Moreover, for samples with high temperature or long reaction time (H-220, H-160-4 and H-160-6), the band at

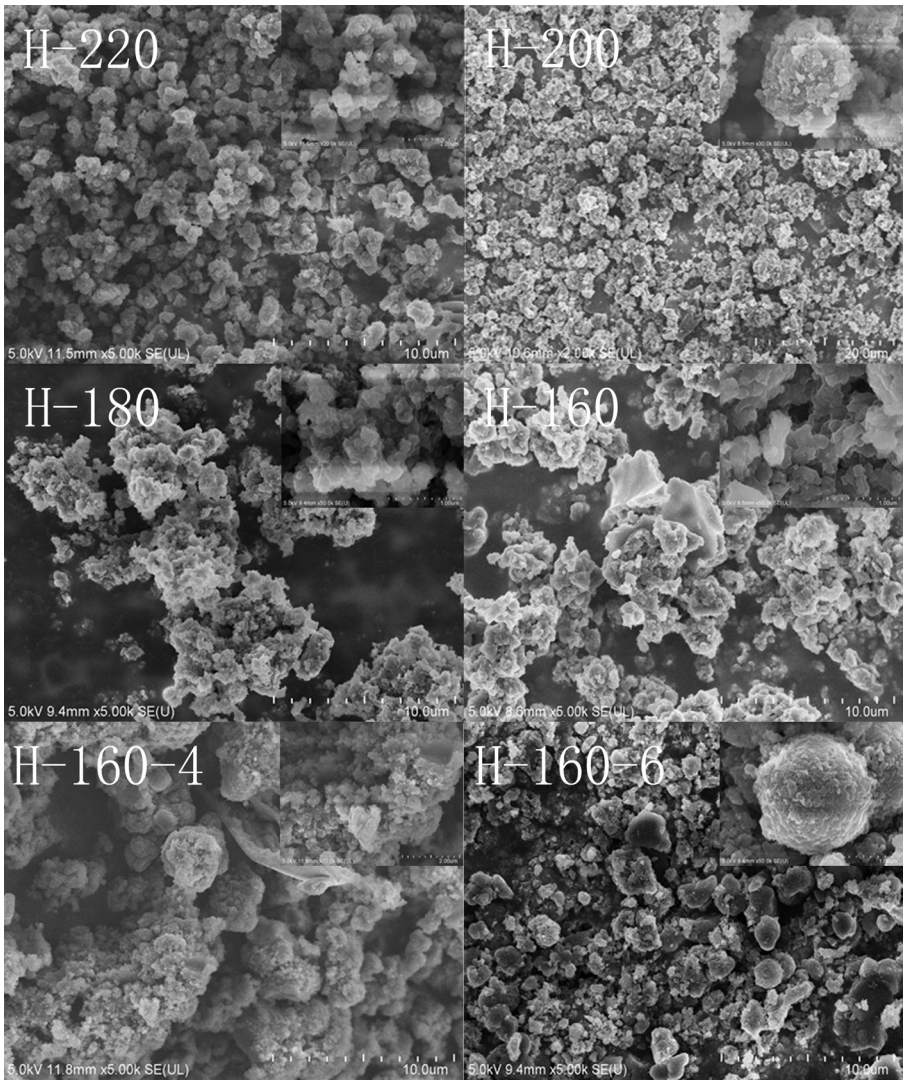

Fig. 1. SEM images of the hydrochar samples.

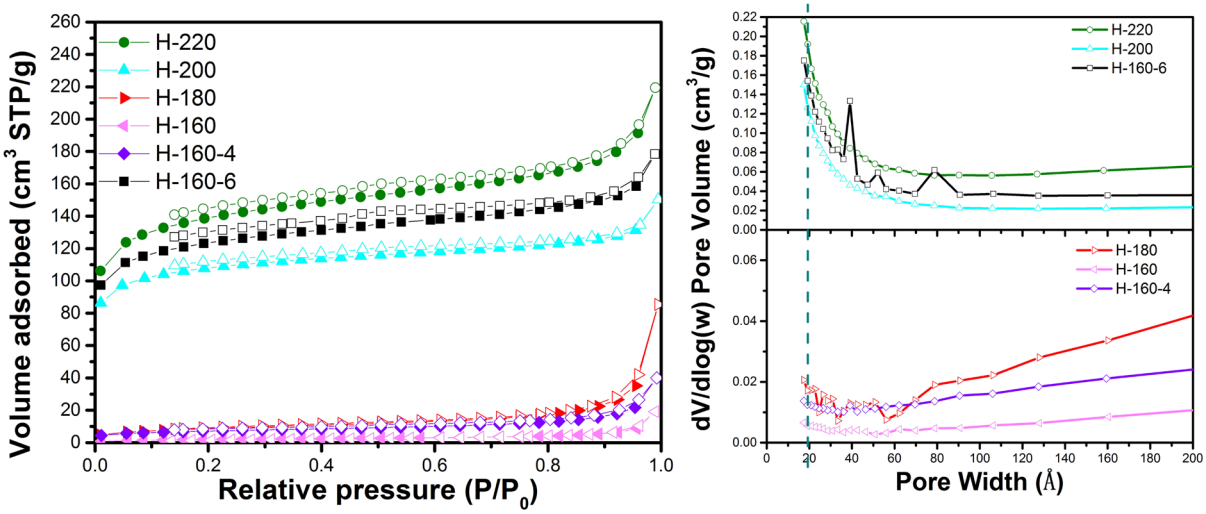

Fig. 2. N_2 adsorption-desorption isotherms and pore size distribution curves of the hydrochar samples.

Table 4
The structural parameters of the hydrochar samples

Sample	S_{BET} (m^2 g^{-1})[a]	V_P (cm^3 g^{-1})[b]	D_P (nm)[c]
H-220	439	0.29	2.6
H-200	329	0.20	2.4
H-180	30	0.05	6.0
H-160	7	0.01	6.3
H-160-4	24	0.03	5.1
H-160-6	388	0.24	2.5

[a] BET surface area (S_{BET}).
[b] Pore volume (V_P) at $P/P_0 = 0.95$.
[c] Pore diameter (D_P).

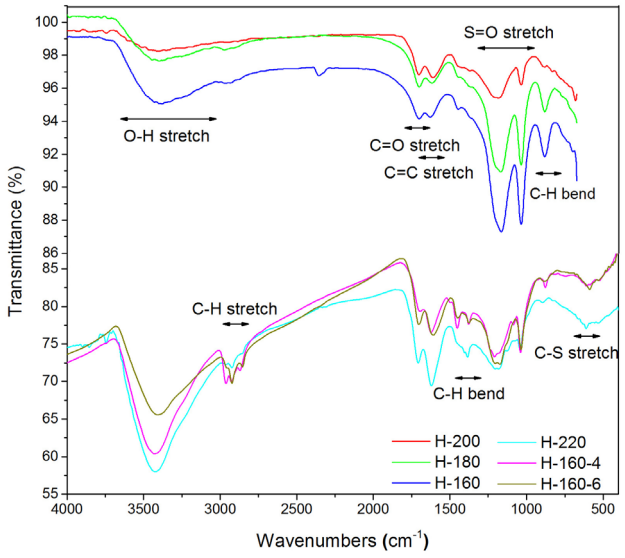

Fig. 3. FTIR spectra of the hydrochar samples.

2930 cm^{-1} represent C–H stretching vibration, which was indicative of aliphatic and aromatics [36]. The bands at 1379 cm^{-1} and 610 cm^{-1} corresponding to the C–H bending vibration and C–S stretching vibration were also found. The number of functional groups on the hydrochar obtained by this experiment was larger than that of the activated carbon [35] and hydrochar prepared by HTC of some organic matters [15,37].

4. Conclusions

The NPEO waste liquid was effectively converted to porous carbon via HTC under the conditions of 0.5 h at 220°C, 0.5 h at 200°C and 6 h at 160°C; the largest BET surface area could reach 439 m^2 g^{-1} at 220°C at 0.5 h. The SEM images showed that the porous carbon had uniform particles and rough surface. The average pore diameter of the hydrochar was concentrated in the mesoporous range close to micropore. Lots of functional groups mainly containing C–H, C=O and S=O existed on the surface of the porous carbon.

Acknowledgments

This work was financially supported by Shanghai Sailing Program (No. 17YF1407200), the "Capacity Building Project of Some Local Colleges and Universities in Shanghai" (No. 17030501200), the Foundation of Shanghai University of Engineering Science (2016-22) and the Project of Shanghai Universities Young Teacher Training Scheme (ZZGCD 16018).

References

[1] G.G. Ying, B. Williams, R. Kookana, Environmental fate of alkylphenols and alkylphenol ethoxylates–a review, Environ. Int., 28 (2002) 215–226.
[2] G.G. Ying, Fate behavior and effects of surfactants and their degradation products in the environment, Environ. Int., 32 (2006) 417–431.
[3] V.K. Sharma, G.A.K. Anquandah, R.A. Yngard, H. Kim, J. Fekete, K. Bouzek, A.K. Ray, D. Golovko, Nonylphenol, octylphenol, and bisphenol-A in the aquatic environment: a review on occurrence, fate, and treatment, J. Environ. Sci. Health, Part A., 44 (2009) 423–442.
[4] N. Bai, R. Abuduaini, S. Wang, M. Zhang, X. Zhu, Y. Zhao, Nonylphenol biodegradation characterizations and bacterial composition analysis of an effective consortium NP-M2, Environ. Pollut., 220 (2017) 95–104.
[5] G. Newcombe, M. Drikas, R. Hayes, Influence of characterised natural organic material on activated carbon adsorption: II. Effect on pore volume distribution and adsorption of 2-methylisoborneol, Water Res., 31 (1997) 1065–1073.
[6] C. Pelekani, V.L. Snoeyink, Competitive adsorption in natural water: role of activated carbon pore size, Water Res., 33 (1999) 1209–1219.
[7] S. Yoshihara, M. Murugananthan, Decomposition of various endocrine-disrupting chemicals at boron-doped diamond electrode, Electrochim. Acta, 54 (2009) 2031–2038.
[8] M. Iqbal, I.A. Bhatti, Gamma radiation/H_2O_2 treatment of a nonylphenol ethoxylates: degradation, cytotoxicity, and mutagenicity evaluation, J. Hazard. Mater., 299 (2015) 351–360.
[9] J. Lu, Q. Jin, Y. He, J. Wu, Biodegradation of nonylphenol polyethoxylates under Fe(III)-reducing conditions, Chemosphere, 69 (2007) 1047–1054.
[10] T. Koottatep, K. Fakkaew, N. Tajai, S.V. Pradeep, C. Polprasert, Sludge stabilization and energy recovery by hydrothermal carbonization process, Renew. Energy, 99 (2016) 978–985.
[11] Q. Zheng, M. Morimoto, T. Takanohashi, Finding of coal organic microspheres during hydrothermal treatment of brown coal, Fuel, 195 (2017) 143–150.
[12] M. Morimoto, H. Nakagawa, K. Miura, Hydrothermal extraction and hydrothermal gasification process for brown coal conversion, Fuel, 87 (2008) 546–551.
[13] R. Dong, Y. Zhang, L.L. Christianson, T.L. Funk, X. Wang, Z. Wang, M. Minarick, G. Yu, Product distribution and implication of hydrothermal conversion of swine manure at low temperatures, Trans. ASABE, 52 (2009) 1239–1248.
[14] B.M. Ghanim, W. Kwapinski, J.J. Leahy, Hydrothermal carbonisation of poultry litter: Effects of initial pH on yields and chemical properties of hydrochars, Bioresour. Technol., 238 (2017) 78–85.
[15] W. Yang, T. Shimanouchi, Y. Kimura, Characterization of hydrochar prepared from hydrothermal carbonization of peels of Carya cathayensis sarg, Desal. Water Treat., 53 (2015) 2831–2838.
[16] N.U. Saqib, M. Oh, W. Jo, S.-K. Park, J.-Y. Lee, Conversion of dry leaves into hydrochar through hydrothermal carbonization (HTC), J. Mater. Cycles Waste Manag., 19 (2017) 111–117.
[17] N.D. Berge, K.S. Ro, J. Mao, J.R.V. Flora, M.A. Chappell, S. Bae, Hydrothermal carbonization of municipal waste streams, Environ. Sci. Technol., 45 (2011) 5696–5703.

[18] M. Goto, R. Obuchi, T. Hirose, T. Sakaki, M. Shibata, Hydrothermal conversion of municipal organic waste into resources, Bioresour. Technol., 93 (2004) 279–284.
[19] D.A.D. Genuino, M.D.G. de Luna, S.C. Capareda, Improving the surface properties of municipal solid waste-derived pyrolysis biochar by chemical and thermal activation: Optimization of process parameters and environmental application, Waste Manage., 72 (2018) 255–264.
[20] S.M. Heilmann, H.T. Davis, L.R. Jader, P.A. Lefebvre, M.J. Sadowsky, F.J. Schendel, M.G. von Keitz, K.J. Valentas, Hydrothermal carbonization of microalgae, Biomass Bioenergy, 34 (2010) 875–882.
[21] L.G. Alba, C. Torri, C. Samorì, J. van der Spek, D. Fabbri, S.R.A. Kersten, D.W.F. Brilman, Hydrothermal treatment (HTT) of microalgae: evaluation of the process as conversion method in an algae biorefinery concept, Energy Fuels, 26 (2012) 642–657.
[22] M. Sevilla, W. Gu, C. Falco, M.M. Titirici, A.B. Fuertes, G. Yushin, Hydrothermal synthesis of microalgae-derived microporous carbons for electrochemical capacitors, J. Power Sources, 267 (2014) 26–32.
[23] S.M. Heilmann, L.R. Jader, M.J. Sadowsky, F.J. Schendel, M.G. von Keitz, K.J. Valentas, Hydrothermal carbonization of distiller's grains, Biomass Bioenergy, 35 (2011) 2526–2533.
[24] Q. Li, Y. Gao, J. Lang, W. Ding, Y. Yong, Removal of Pb(II) and Cu(II) from aqueous solutions by ultraviolet irradiation-modified biochar, Desal. Water Treat., 82 (2017) 179–187.
[25] M.A. Islam, I.A.W. Tan, A. Benhouria, M. Asif, B.H. Hameed, Mesoporous and adsorptive properties of palm date seed activated carbon prepared via sequential hydrothermal carbonization and sodium hydroxide activation, Chem. Eng. J., 270 (2015) 187–195.
[26] J. Poerschmann, B. Weiner, I. Baskyr, Organic compounds in olive mill wastewater and in solutions resulting from hydrothermal carbonization of the wastewater, Chemosphere, 92 (2013) 1472–1482.
[27] J. Poerschmann, B. Weiner, S. Woszidlo, R. Koehler, F.-D. Kopinke, Hydrothermal carbonization of poly(vinyl chloride), Chemosphere, 119 (2015) 682–689.
[28] B. Weiner, I. Baskyr, J. Poerschmann, F.-D. Kopinke, Potential of the hydrothermal carbonization process for the degradation of organic pollutants, Chemosphere, 92 (2013) 674–680.
[29] Y. Ge, W. Zhang, G. Xue, J. Zhao, Carbonization of chlorinated organic residual liquid for energy source generation, J. Mater. Sci. Chem. Eng., 3 (2015) 95–103.
[30] M. Kruk, M. Jaroniec, Gas adsorption characterization of ordered organic-inorganic nanocomposite materials, Chem. Mater., 13 (2001) 3169–3183.
[31] P. Gao, Y. Zhou, F. Meng, Y. Zhang, Z. Liu, W. Zhang, G. Xue, Preparation and characterization of hydrochar from waste eucalyptus bark by hydrothermal carbonization, Energy, 97 (2016) 238–245.
[32] Y. Ge, W. Zhang, G. Xue, P. Rao, Hydrothermal carbonization of nonylphenol ethoxylates waste liquid for energy source generation, Am. J. Anal. Chem., 6 (2015) 1059–1066.
[33] Y. Huang, W. Liu, W. Wang, Q. Feng, J. Liu, Synthesis of a carbon@Rectorite nanocomposite adsorbent by a hydrothermal carbonization process and their application in the removal of methylene blue and neutral red from aqueous solutions, Desal. Water Treat., 57 (2015) 13573–13585.
[34] J. Mosa, A. Durán, M. Aparicio, Sulfonic acid-functionalized hybrid organic-inorganic proton exchange membranes synthesized by sol-gel using 3-mercaptopropyl trimethoxysilane (MPTMS), J. Power Sources, 297 (2015) 208–216.
[35] M. Li, W. Li, S. Liu, Hydrothermal synthesis, characterization, and KOH activation of carbon spheres from glucose, Carbohydr. Res., 346 (2011) 999–1004.
[36] Y. Gao, X. Wang, J. Wang, X. Li, J. Cheng, H. Yang, H. Chen, Effect of residence time on chemical and structural properties of hydrochar obtained by hydrothermal carbonization of water hyacinth, Energy, 58 (2013) 376–383.
[37] M. Xie, K. Fang, Y. Shen, Y. Wang, J. Liang, L. Peng, X. Guo, W. Ding, Catalytic hydroxylation enables phenol to efficient assembly of ordered mesoporous carbon under highly acidic conditions, Micropor. Mesopor. Mater., 223 (2016) 114–120.